Journal of *Marine Science and Engineering*

MDPI

Article

Design Process and Advanced Manufacturing of an Aquatic Surface Vehicle Hull for the Integration of a Hydrogen Power Plant Propulsion System

Jordi Renau Martínez [1,*], Víctor García Peñas [1], Manuel Ibáñez Arnal [1], Alberto Giménez Sancho [1], Eduardo López González [2], Adelaida García Magariño [3], Félix Terroba Ramírez [3], Francisco Javier Moreno Ayerbe [3] and Fernando Sánchez López [1]

[1] Escuela Superior de Enseñanzas Técnicas, Universidad Cardenal Herrera—CEU Universities, C/San Bartolomé 55, 46115 Alfara del Patriarca, Valencia, Spain
[2] Área de Energía y Medio Ambiente—Laboratorio de Energía de El Arenosillo, Instituto Nacional de Técnica Aeroespacial (INTA), Ctra. Juan. Matalascañas, km34, 21130 Mazagón, Huelva, Spain
[3] Instituto Nacional de Técnica Aeroespacial "Esteban Terradas", Subdirección General de Sistemas Navales, Ctra. de la Sierra s/n, 28048 El Pardo, Madrid, Spain
* Correspondence: jordi.renau@uchceu.es

Abstract: This article presents the design and manufacturing of a hydrogen-powered unmanned aquatic surface vehicle (USV) hull. The design process comprised three stages: (1) defining the requirements for a preliminary geometry, (2) verifying the hydrodynamic hull performance using computational fluid dynamics (CFD) simulations, and (3) experimentally validating the hydrodynamic hull performance and CFD analysis results through experimental fluid dynamics in a calm water towing tank. The manufacturing process utilized additive manufacturing technologies, such as fused granular fabrication and selective laser sintering, to produce the hull and other components, including the propeller and the rudder; thermoplastic materials with carbon fiber reinforcement were employed. The experimental results demonstrate that the optimized trimaran hull exhibited low hydrodynamic resistance (7.5 N), high stability, and a smooth flow around the hull (up to 2 m/s). The design and manufacturing of the USV hull met expectations from both hydrodynamic and structural perspectives, and future work was outlined to integrate a power plant, navigation system, and scientific equipment.

Keywords: trimaran hull; USV hull design; 3D printing manufacture; hydrogen; experimental fluid dynamics

Citation: Renau Martínez, J.; García Peñas, V.; Ibáñez Arnal, M.; Giménez Sancho, A.; López González, E.; García Magariño, A.; Terroba Ramírez, F.; Moreno Ayerbe, F.J.; Sánchez López, F. Design Process and Advanced Manufacturing of an Aquatic Surface Vehicle Hull for the Integration of a Hydrogen Power Plant Propulsion System. *J. Mar. Sci. Eng.* **2024**, *12*, 268. https://doi.org/10.3390/jmse12020268

Academic Editor: Decheng Wan

Received: 22 November 2023
Revised: 22 December 2023
Accepted: 4 January 2024
Published: 1 February 2024

1. Introduction

Interest is growing in the development of unmanned vehicles, which are vehicles that are operated without a crew and can be either remotely piloted or autonomous, depending on the degree of automation [1]. Unmanned marine vehicles can be divided into unmanned underwater vessels (UUVs) and unmanned surface vehicles (USVs). The hydrodynamic characteristics of UUVs have been reviewed recently [2], and the optimization of their hulls [3] has been performed for different operational conditions such as navigation at snorkeling depth [4] or for exploration in the Caribbean Sea [5]. Research and development on USVs focus not only on typical lightweight applications, like ocean research [6] or wetland monitoring tasks [7–9], but also on human transportation [10]. Aquatic vehicles compete with other unmanned vehicles in dangerous applications such as disaster scenes and surveillance tasks at borders, sensitive areas, and ports [11–13]. A review of USVs up to 2016 was written by Liu et al. [14], in which the main USV developments are shown. In this review, a table summarizing the 33 different USVs used in published research is displayed, showing the research purpose of each USV. According to this table, only one USV (named

MIMIR) was dedicated to shallow water research. This indicates that although further research involving USVs in shallow waters has been performed since then, for example, by Kang et al. [13], few USVs have been designed for operation in shallow water. In this context, this paper is dedicated to improving the design of a USV intended to be operated in shallow water.

The developments of and challenges facing USVs can also be found in the review of Liu et al. [14]. According to Liu et al. [14], the basic elements of every USV are (1) the hull and structural elements, (2) the propulsion and power system, (3) the guidance and navigation control system, (4) the communications systems, (5) the data collection system, and (6) the ground station. In recent years, many published papers dedicated to USV GNC and communication systems have looked at motion planning [15], trajectory optimization [16], obstacle avoidance [17], and the control of multiple USVs [18–20], among others. Regarding the hull and structural design, three types of optimization can be performed, according to Meng et al. [21]: topology optimization, size optimization, and shape optimization. A review on topology optimization methods for additive manufacturing was conducted by Zhu et al. [22]. Recently, Wu et al. [23] proposed a method for optimizing the external shape and the internal unit cells of a hull simultaneously. However, in the marine context, the external shape of a hull is responsible for its drag, and therefore, the hydrodynamic performance of the hull's design needs to be considered [24,25]; such performance can be evaluated using CFD methods but also needs to be validated through experimental hydrodynamic tests [26]. Moreover, although research efforts regarding propulsion and power systems are mainly focused on the development of a vehicle power plant and its optimal control, a vessel's energy consumption is intimately related to the hull design. Finally, cost reduction has been studied recently by Setiawan et al. [27], who proposed the design, manufacturing, and development of an affordable USV for Indonesia. In this context, the manufacturing process is also relevant in reducing costs.

The main objective of the present research paper is to present and describe not only an improved design and manufacturing process but also a final geometrical experimental validation of a 3D-printed hull for a hydrogen-powered autonomous unmanned aquatic surface vehicle. The USV is destined to operate in freshwater reservoirs and shallow waters, incorporating sensors and scientific equipment to monitor physical, chemical, and biological parameters. In designing a hydrogen-powered autonomous unmanned aquatic surface vehicle (USV) hull, the project follows four specific guidelines as its design framework: (1) The design aims for a simple hull construction, making production easy and ensuring spare parts are readily available. (2) The design must support long-endurance missions (~12 h). (3) The system's scalability is crucial, and the use of a hydrogen-based power plant means different mission needs can be handled due to hydrogen's large specific energy ratio. (4) The hull should also prioritize energy efficiency, focusing on low-friction and low-speed capabilities to make the most of the produced energy during long missions. These guidelines emphasize our commitment to a practical, sustainable, and adaptable USV hull.

The outline of this paper can be summarized as follows: In Section 2, the design methodology, software, and experimental facilities are described. Section 3 outlines the design process, and the experimental results are also discussed. Finally, Section 4 summarizes the main conclusions and outlines future work.

2. Materials and Methods

The USV design process was based on a three-phase methodology (Figure 1). Firstly, we defined a primary geometry using literature and technical reviews, aiming to satisfy all the requirements and mandatory design conditions. Secondly, the defined geometry was analysed and validated using a computational numerical hydrodynamics simulation (computational fluid dynamics, CFD). Finally, the hull geometry was manufactured and experimentally validated in a calm water towing tank facility.

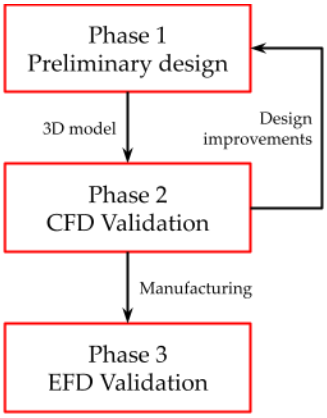

Figure 1. Three-phase hull design methodology.

2.1. Computational Fluid Dynamics (CFD) Software

The CFD analysis was performed with the commercial software ANSYS CFX (ver.: 2021R1). This CFD software is a computer-aided engineering software tool used to help in the iterative hull design process, specifically by parametrizing the vessel dimensions to obtain the best technical solution that fits all requirements. This CFD software simplifies the comparison between different hull designs by analyzing and visualizing different variables to improve the final design and to ensure a low drag force in order to achieve the required propulsion power. These variables are the ship's resistance, the dynamic pressure distribution on the hull's surface, the streamlines, the hull skin's friction, and the wave elevation around the ship. The domain was meshed with 'ANSYS Meshing', employing an unstructured meshing approach around the hull to capture its geometry, especially its curvature, and a structured mesh was used for the outer domain. This choice enhances accuracy since the flow direction is well known. A RANS method was used with a k-w SST turbulence model.

2.2. Experimental Fluid Dynamics (EFD) Validation

The experiments were conducted in the calm water towing tank at INTA-CEHIPAR (Spain), which is 320 m long, 12.5 m wide, and 6.5 m deep. Images of the facility are shown in Figure 2. The facility includes a towing carriage capable of testing models at speeds up to 10 m/s with a maximum acceleration of 1 m/s^2. A resistance test was performed in which the model's resistance and speed through the water were simultaneously measured. The prototyped hull was secured to the towing carriage by a towing dynamometer, and only the horizontal tow force was measured. Two guides prevented sway (translation on the Y-axis) and yaw (rotation on the Z-axis) movements. The carriage accelerated the hull along the calm water tank, recording the force necessary to achieve and maintain the set speed. The experimental measurements included the hull resistance, sink, and trim of the ship.

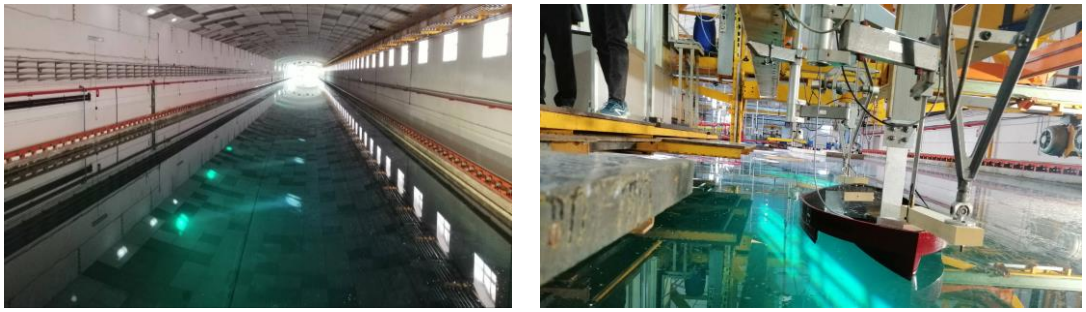

Figure 2. Calm water towing tank facility (CEHIPAR-INTA).

2.3. Manufacturing Technology and Materials

The use of composite materials is the preferred approach to reducing component weight in the sustainable transport industry, driven by energy efficiency requirements. While these materials excel in terms of mechanical behavior, their surface resistance to atmospheric agents, mechanical stress, and chemical exposure requires optimization, especially in aquatic or marine applications. Additive manufacturing technologies (AMTs or 3D printing) offer the ability to utilize diverse materials and manufacturing strategies in a single device. Compared to subtractive technologies, the key advantage of AMT lies in its optimal raw material use and the potential for more efficient products with complex and lightweight geometries, facilitated by topological optimization [28]. This manufacturing process is highly flexible due to extensive parametrization. Moreover, 3D printing technology provides a variety of materials suitable for naval component construction, including high-performance thermoplastics such as acrylonitrile butadiene styrene (ABS), polylactic acid (PLA), polyethylene terephthalate glycol (PETG), and polyamides (PAs). These materials contribute to durability, strength, and a favorable strength-to-weight ratio.

There are over twenty different 3D printing technologies available, with some of the most common ones being fused deposition modeling (FDM), stereolithography (SLA), and selective laser sintering (SLS) [29]. Among these methods, the fused deposition modeling (FDM) system is the most widely used, and it has become indispensable in prototyping and even in final component production across various industries, including naval applications [30,31]. An advanced variant of the FDM process is the fused granule fabrication (FGF) system, an additive forming process seeing significant growth in its industrial application. This technology combines the superior attributes of injection molding components with the manufacturing flexibility of 3D printing. The FGF machine, a numerically controlled piece of equipment (CNC), has three degrees of freedom for positioning the extrusion head and a fourth degree of freedom for controlling the rate of material deposition. The manufactured piece is formed on a static platform as the material is extruded through the nozzle over the platform, layer by layer. After each finished layer, the extrusion nozzle moves up, and the next layer is added on top of the previous one. The nozzle can tilt up to 45° away from the vertical axis to avoid supporting structures and create parts with overhangs, reducing waste and manufacturing time. FGF is suitable for the fabrication of medium to large parts featuring thick walls and low-complexity geometries. The technology has a productivity of up to 10 kg/h, which is a key factor in manufacturing large parts, especially when post-processing, e.g., by CNC machining, is necessary. Additionally, FGF can use specialized plastic composites, incorporating properties like fire resistance, chemical resistance, or electrical conductivity, depending on specific application requirements. For this research, the selected technology was the FGF system, and the material used was LNP™ THERMOCOMP™ AM COMPOUND AC004XXAR1, supplied by Sabic (Riyadh, Saudi Arabia). This thermoplastic material, a compound based on acrylonitrile butadiene styrene (ABS) polymer containing 20 wt.% carbon fiber, adds features such as a higher stiffness, easier processing, low warp, and a good print surface quality. Moreover, lower shrinkage during cooling ensures greater dimensional stability and less thermal expansion during the part's use, making it a suitable material meeting the defined requirements for manufacturing the ship's hull.

3. Results and Discussion

This section outlines the design process and the experimental validation of the USV in three separate subsections. Section 3.1 explains the preliminary design and the reasoning for selecting a trimaran geometry, which was based on a literature review and considering standard ship profiles adapted to the proposed USV's scale. Section 3.2 reports the results of the CFD analysis to ensure the hydrodynamic requirements (e.g., low resistance) for the hull geometry are complied with before manufacturing. Finally, Section 3.3 presents the fabrication results and the experimental validation of the final geometry.

3.1. First Design Stage: Requirements and Preliminary Design

The proposed USV will perform low-speed missions in freshwater reservoirs and shallow lakes, incorporating sensors and scientific equipment to monitor physical, chemical, and biological parameters. The proposed design must meet the requirements of the manufacturing process, as well as the design framework laid out in Section 1, to ensure that the hull can seamlessly integrate all systems and devices necessary for mission success. These systems include (1) the power plant, (2) the navigation system, and (3) all scientific equipment and sensors.

The power plant is based on hydrogen and battery hybridization, aligning with the research framework's objective. This hybrid power plant enhances the USV's autonomy, optimizing both its specific power and energy, as was experimentally validated by the research team [32]. The navigation system relies on an embedded computer with a robotic operational system (ROS). The navigation system is responsible for governing the USV, controlling the mission's activities and scientific measurements, and managing the USV's trajectory and communications, but does not control the power plant itself. Both systems collaborate, sharing information and telemetry. The initial mechanical design of the propulsion and vessel direction system involves a single propeller and a double-bladed rudder, both regulated by electrical servomotors ensuring precise system positioning.

The USV hull design took into consideration both a state-of-the-art review and the specific operational needs of the proposed vehicle. The final prototype hull size was constrained by the need for it to fit in a standard car trunk (1300 $\times$ 960 $\times$ 585 mm), keeping in mind the commitment to practicality and scalability. This decision regarding size does not restrict other decisions made for the current prototype, which must easily apply to a larger version in the future. However, scaling up this prototype would require larger transportation methods and a modified launch strategy. Despite these changes, the components, their distribution, and the fundamental geometry would remain consistent, demonstrating the adaptability of our design approach.

The four key requirements guiding the prototype hull's design process are as follows:

1. Optimal solar panel integration: The design aims to make the working deck as big as possible in relation to the ship's size. This has two benefits: it helps with fitting all systems aboard and prepares the ship for the addition of solar panels later on.
2. Balanced seakeeping and stability: Balancing seakeeping and stability is crucial for long-duration missions, as specified. Placing the ship's center of mass low, while keeping in mind the limitations of gyroscopic stabilization, is a perfect balance between seakeeping and stability.
3. Single propulsion system: A propulsion system consisting of a motor, shaft, and propeller ensures simplicity in construction and efficient operation and control.
4. Low hydrodynamic resistance: The hydrodynamic resistance of the USV hull should be as low as possible to reduce the power requirements necessary for navigation.

To summarize, these constraints are not just important guidelines during the design phase, but they also reinforce the researchers' strong dedication to the specifications outlined in the project's initial design framework. This combination ensures a coherent approach that matches the details of the hull's design with the overarching goals stated in the initial conditions.

A sample of the various hull models developed in the vehicle design process is presented in Figure 3, and the main advantages and disadvantages of each model are outlined in Table 1. Figure 3 shows the models arranged based on the evolution of the designed hull typology. The process followed a natural progression from a monohull to a multihull vehicle, achieving the correct positioning of interior components to achieve high stability, which is essential for unmanned vehicles.

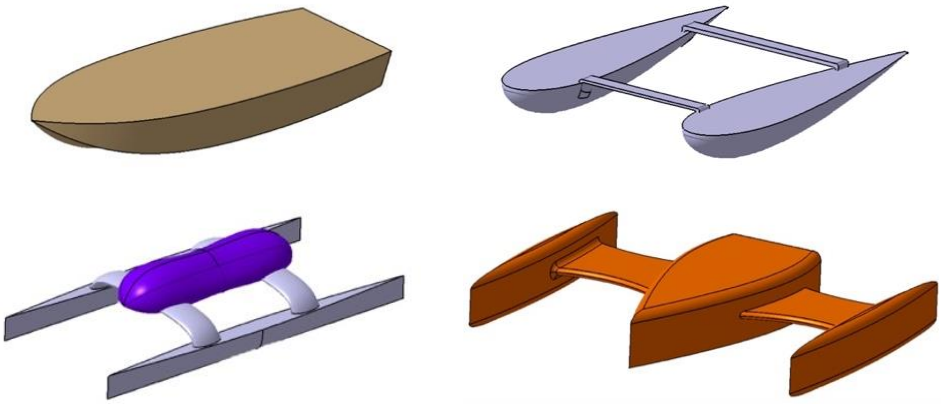

Figure 3. USV hull design evolution from a monohull to a trimaran geometry.

Table 1. Main advantages and disadvantages for different hull designs and interest parameters.

	Monohull	Catamaran	Trimaran
Deck surface [1]	Small	Large	Large
Seakeeping and stability	Medium	High	High
Implementation of a single power axis	Implemented appropriately	Not implemented properly	Implemented appropriately

[1] Surface defined as the available space for a maximum boat length.

The monohull, according to geometry, is stable but requires greater material consumption. The catamaran geometry is a very good solution and is widely used in the literature [33], but in manufacturing, it loses points against the monohull since it requires a greater number of manufacturing steps because of its separate hulls. The requirement of implementing a single power plant and line of axles makes the trimaran option more suitable than the catamaran. Likewise, with this configuration, the propulsion plant can be located in the bay and on the lower decks, which places the vertical center of mass in a lower position than that in the catamaran option, in which the propulsion system would have to be located on the main deck. For all these reasons, and with the aim of innovating in the development of USVs, it was decided to increase the USV's stability by developing a trimaran hull. The trimaran design allows the navigation speeds to be increased without increasing the complexity of manufacturing or the consumption of material, as is the case in military applications, both in terms of defense and surveillance [34].

For the preliminary design of the trimaran, the state of the art was taken into account. Recent investigations on the design of trimaran have researched the structure [35–38], the outrigger layout [39–42], optimization to reduce resistance [42–45], seakeeping and stability performances [46–48], and the design method itself [49–51]. From a structural point of view, Daidola et al. [35] discussed preliminary structural design procedures for a large high-speed sealift trimaran, while Tang et al. [36] applied structure monitoring technology, and Jia et al. [37] proposed a lightweight design of a trimaran bulkhead using structural topology optimization. According to Khoob et al. [38], for a wave-piercing trimaran, transverse torsion moments and shear forces are significant in head seas, while transverse bending moments have larger response magnitudes in oblique seas.

The outrigger layout, which refers to the longitudinal and transverse distance between the main hull and the two outriggers, can be optimized to reduce the interference wave resistance between the main hull and the outriggers by means of both numerical [39] and experimental studies [41]. The results of Ghadimi et al. [39] showed that trimaran vessels have suitable dynamics with lower longitudinal side bodies and large transversal distances, which was also confirmed by the work of Sun et al. [52], in which the flow field between the main hull and demihull can be observed. Moreover, Khoob et al. [41] concluded that symmetric side hull shapes had better performance in terms of total resistance than inboard or outboard shapes. Therefore, these last two considerations were taken into

account in the preliminary design of the USV. Additionally, some investigations exist on the hydrodynamics and aerodynamic characteristics of the tunnel, such as the studies of Jiang et al. [53,54] or Ding et al. [55].

Different methods have been used in the literature to predict the resistance of the trimaran and optimize its performance by reducing resistance. In 2015, Wang et al. [42] proposed a fast numerical method to predict the wave resistance of a trimaran hull, while Tang et al. [43], in 2020, studied a new three-dimensional, non-linear time-domain Rankine–Green method to calculate the wave load. Recently, Xu et al. [44] proposed an empirical estimation formula of the resistance coefficient based on multiple regression analysis, and Yao et al. [45] proposed a hybrid Green function method to calculate the added resistance. Additionally, hull form optimization has been performed using the self-blending method combined with CFD [49] and using multi-objective optimization based on CFD studies [50]. According to Nazemian et al. [51], the longitudinal center of buoyancy and block coefficient have significant effects on the total resistance. From the literature, it can be inferred that CFD analysis seems to be an adequate tool for performing hull optimization.

Furthermore, Liao et al. [46] investigated the seakeeping performances of trimaran hulls by means of CFD prediction, concluded that the behaviors of seakeeping and slamming differ significantly from those of monohull ships, and reported severe bow slamming and green water in oblique waves. Gong et al. [47], who also recently studied the seakeeping of trimarans, observed that the sailing speed has less influence on the motion than on the added resistance, especially in head and oblique waves. Finally, an example of seakeeping optimization in trimaran hulls was conducted by Wang et al. [48], who used a fast elitist non-dominated sorting genetic algorithm to optimize the outrigger layout.

Considering the available information in the literature and the authors' expertise, a first hull geometry was proposed from standardized profiles. For a mission speed of 1 m/s, the hull length was approximately 1 m, with a beam of 0.6 m and a prop of 0.3 m. The total mass displacement was ca. 20 kg with a draft of 0.12 m.

3.2. Second Design Stage: CFD Analysis

The CFD analysis of the unmanned marine vehicle hull was performed using a Froude number of 0.316 and a Reynolds number of 1.14×10^6 using ANSYS CFX software, which has been verified in the past for similar geometries. The water and air flows around the hull were simulated by solving the two-phase and free surface problems using the VOF (volume of fluid) method. A steady-state analysis was performed, using the RANS method, with a k-w SST turbulence model. The advection scheme and turbulence value were set to a high resolution and coupled with the volume fraction. A mesh with hexahedral and tetrahedral elements was generated using linear elements with zero degrees of freedom since the expected sinkage and trim were very small. Moreover, an inflation strategy was applied near the hull's surface to calculate the boundary layer. The boundary layer was chosen to obtain a more accurate resistance value via the better modeling of the frictional resistance. In the turbulence model used, the treatment of the near-wall flow is highly dependent on the y+ parameter. To avoid the use of wall functions in modeling the boundary layer, this parameter must be equal to or less than 1, so y+ = 1 was set as the target, eliminating the need for wall functions. The boundary conditions, the multiphase problem characteristics, the convergence criteria, and the number of partitions for the calculation were defined. For the design speed, a grid performance test was conducted for which a total of six meshes were tested with different numbers of elements (Figure 4).

The results of the resistance, the dynamic pressure coefficient, the Meissner effect, and the wave elevation around the hull were obtained. It was observed that the resistance level was low (about 7.2 N) and there were no phenomena of inversion or flow detachment at the stern. Therefore, the power required for the bare hull (without appendices and without a load on board) for displacement at a constant speed of 1 m/s was only 7.2 W. The streamlines, the wave profile, and the pressure distribution in the hull, all of which are depicted in Figure 5, showed a smooth and uniform flow around the hull. The

dimensionless dynamic pressure coefficient and the wave elevation indicated that the hull had a low drag and a small wake. The expectations from the hydrodynamic point of view were to obtain a design with low resistance so that the fuel cell installed would have a large power margin not only to provide the required propulsion, but also to supply power for ancillary consumption. As a consequence of these results, it was concluded that the design of the hull met these expectations.

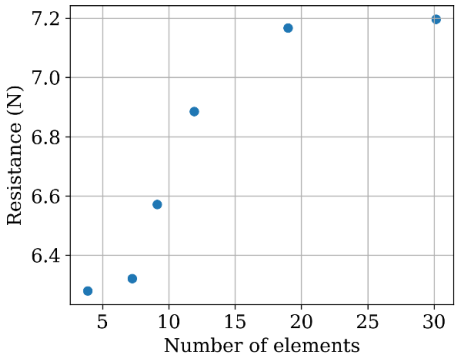

Figure 4. Convergence of the resistance test with different meshes.

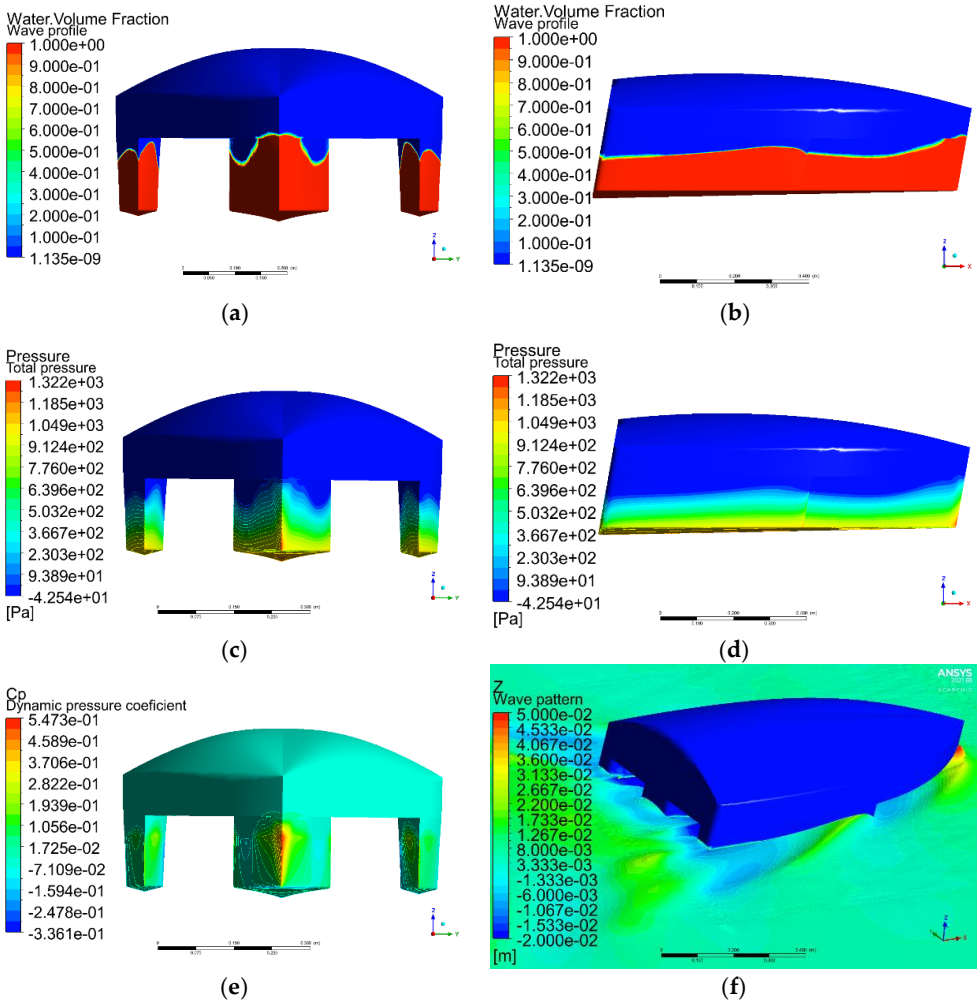

Figure 5. Graphical results from the CFD analysis. (**a**,**b**) The wave profile; (**c**,**d**) the pressure distribution along the hull; (**e**) the dynamic pressure coefficient, Cp; (**f**) the generated wave train.

3.3. Third Design Stage: Manufacturing and Experimental Validation

In this section, we present the manufacturing process and the experimental validation. Section 3.3.1 details the hull's fabrication, while Section 3.3.2 focuses on the experimentation conducted at the calm water towing tank facility, including the obtained results.

3.3.1. Manufacture of the Vessel's Hull

The vessel was manufactured via direct extrusion using a fused granular fabrication (FGF) system with an 8 mm nozzle and a reinforced ABS polymer with 20 wt.% carbon fibers. Figure 6a,b show the 3D printing process of the trimaran hull. The entire hull was printed without any infill or support structure, minimizing material waste. The coating was applied as a specialized finish to provide environmental protection against UV radiation, humidity, corrosion, surface impacts, waves, and other factors. Additionally, it was applied to minimize the hydrodynamic resistance coefficient.

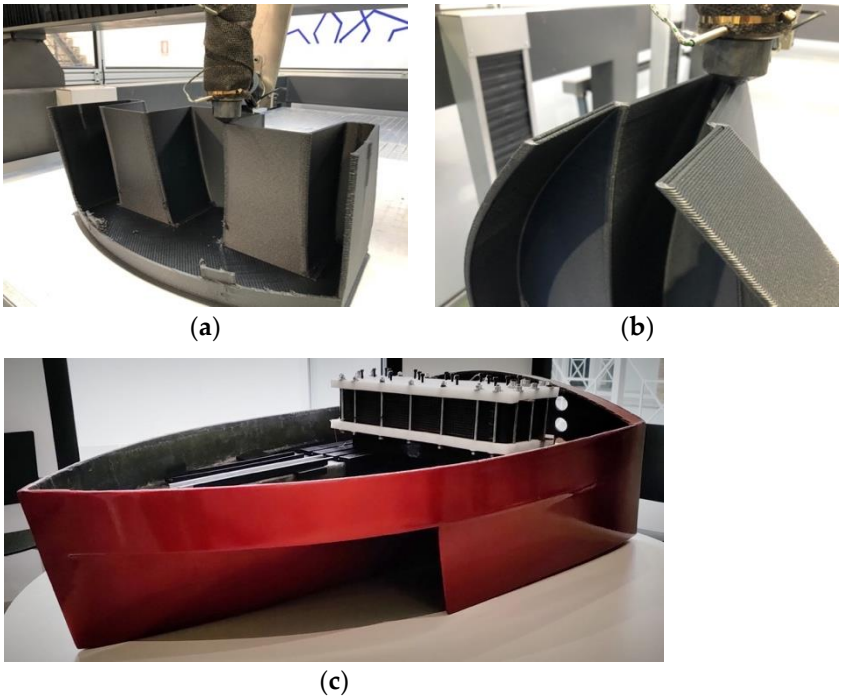

(**a**) (**b**)

(**c**)

Figure 6. USV hull manufactured with FGF technology. (**a**) Details of the 3D printing process; (**b**) details of the double layer that forms the hull; (**c**) finished hull in the first stage of power plant integration.

The manufacturing technology parameters needed to be optimized as a function of the material, geometry, and desired mechanical properties of the final piece. Therefore, fabrication was performed and the adherence and resistance of the finished product were tested and validated by the authors [56]. Figure 6a,b show the hull being manufactured. Figure 6c depicts the final hull after coating.

Other mechanical components, such as the propeller (Figure 7a) or the rudder, were also manufactured using additive manufacturing technologies, employing polyamide polymer and selective laser sintering (SLS) equipment (Sinterit Lisa SLS). This technique produces parts with lower densities and higher porosities, but with better mechanical properties for underwater applications [29]. The high porosity of the sintered PA material was tested for water absorption. The pieces were submerged in a water container, and their mass and dimensions were measured before and after the immersion in several moments, as depicted in Figure 7b. The results showed that the part increased in mass by 13 wt.% due to water absorption but did not exhibit any significant dimensional change, which is the most important parameter for maintaining the functionality of the component.

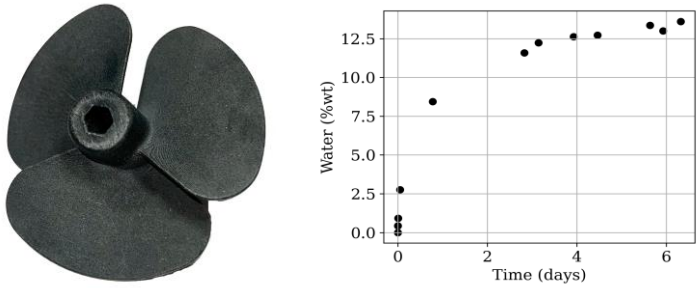

(**a**) (**b**)

Figure 7. Mechanical components manufactured with SLS 3D printing technology. (**a**) Manufactured USV propeller; (**b**) polyamide water absorption test results.

3.3.2. Hydrodynamic Experimental Validation

The experimental fluid dynamics (EFD) analysis was conducted on the CFD-optimized hull. The aim was to compare and experimentally validate the CFD optimization process. The hull was tested at full scale in the calm water towing tank, so it was not necessary to apply any extrapolation to the experimental results. Figure 8 depicts the test setup. Figure 8a,b present the hulls tested during the experimentation and depict the front and rear views of the tested hull. Figure 8c illustrates how the load sensor was installed into the real hull to simulate a similar propelling force. The experimental setup was a ship's draft of 12 cm with a static trim of zero degrees.

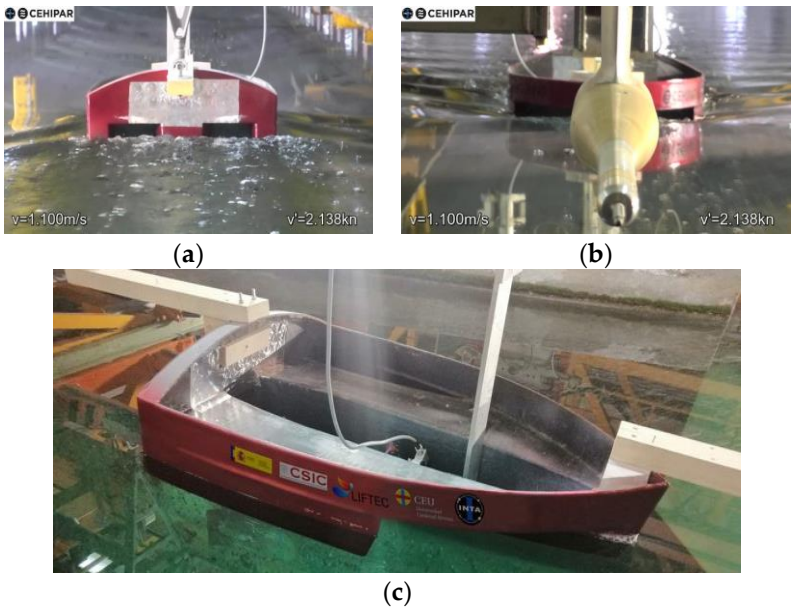

(**a**) (**b**)

(**c**)

Figure 8. USV setup on the tow truck in the CEHIPAR facility. (**a**) Backside view; (**b**) frontside view; (**c**) lateral view (static position), where the load sensor position is shown.

The set of experiments was performed on the final USV hull. The experimentation speed ranged from 0.4 to 2.0 m/s, which was 1 m/s over the rated speed of the ship due to the well-behaved nature of the hull during the experimentation.

The hydrodynamic resistance, the ship trim angle, and the bow and stern draft were measured in the experiments. The results are shown in Figure 9. The experiments with the optimized hull focused on the stability of its navigation. The speed was increased until the outrigger hulls generated a wave train that interfered with the main hull's leading edge, compromising the stability of the trimaran at speeds above 2 m/s. Figure 9 incorporates experimental data obtained from tests conducted on the uncoated hull (blue stars), facilitating

a comparison of the coating's advantages and illustrating the hydrodynamic improvement achieved by the ship due to the smoother surface created by the finishing coating.

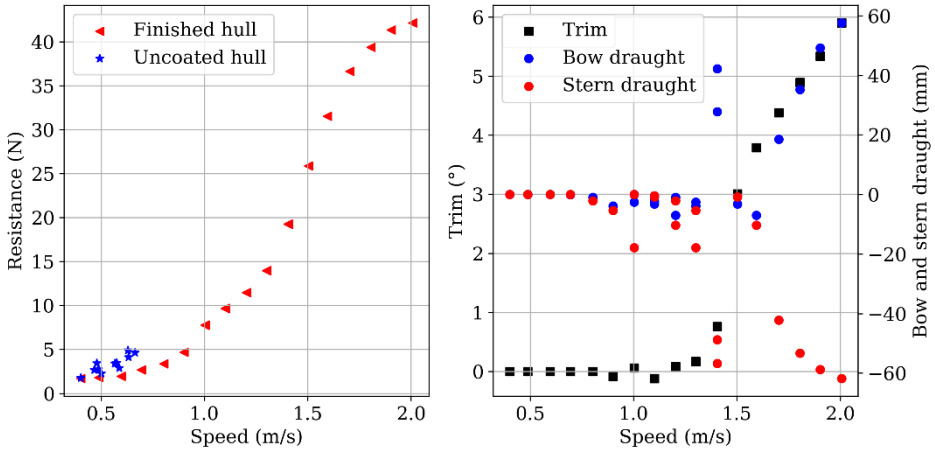

Figure 9. Experimental results for the hull resistance at constant speed. Measured in the calm water towing tank at CEHIPAR facilities.

The optimized hull demonstrated excellent hydrodynamic performance across all speed ranges, demonstrating a low resistance force of 7.5 N at the rated speed of 1 m/s. Table 2 shows the CFD and EFD results and their deviation percentage.

Table 2. Comparison of CFD and EFD results.

Speed (m/s)	EFD Resistance (N)	CFD Resistance (N)	Deviation CFD vs. EFD
0.8	3.7	3.5	4.7%
1.0	7.5	7.2	5.3%
1.2	11.9	10.9	8.9%

It can be observed that the deviation in CFD results with respect to the EFD results is less than 10% for the tested velocities, thus validating the CFD results and showing that, for the designed velocity (1 m/s), the deviation is only on the order of 5%. The disparities between the CFD and EFD results primarily stem from flow shedding at the stern, which was not captured in the CFD simulations but occurred in the experimental tests. Nevertheless, this still translates to a remarkably low propulsion power of 7.5 W to maintain a steady speed while keeping the trim angle close to the horizontal position.

At higher speeds, the ship exhibited a trim angle of 6°, with the bow and stern draft measuring 58 mm and −62 mm, respectively.

4. Conclusions and Future Work

This paper reported the design process and advanced manufacturing of a hull for an aquatic unmanned surface vehicle (USV) powered by a hydrogen propulsion system. The design process unfolded in three stages: (1) the creation of a preliminary design aligned with state-of-the-art USV requirements in order to accommodate a future hydrogen power plant and ensure easy transportation; (2) conducting a CFD analysis validating the preliminary hull's geometry and proposing minor adjustments if necessary; and (3) manufacturing and experimental validation of the final hull geometry in a calm water towing tank, verifying the CFD analysis and confirming the expected hydrodynamics with low drag resistance.

The effectiveness of the CFD analysis was underscored by its accurate prediction of low hydrodynamic resistance, a validation confirmed through experimental fluid dynamic tests. The final hull geometry guaranteed low drag, fostering a smooth and uniform water flow around the hull, meeting the hydrodynamic criteria. At the rated speed (1 m/s), the measured resistance was 7.5 N, translating to a low propulsive power of 7.5 W. While this

presented a minor deviation from the predicted CFD value of 7.2 N (less than 5.3%), it is crucial to note that the experimental value should align with the power plant, accounting for potential higher power losses due to energy chain inefficiencies; however, these considerations are beyond the present paper's scope.

The successful and innovative design and manufacturing of the hull, particularly in the trimaran configuration, has a demonstrated suitability for USV applications, ensuring stability and facilitating the installation of all required systems. Future efforts will center on integrating the power plant and navigation system and evaluating the USV's performance in real-world scenarios.

Author Contributions: Conceptualization, J.R.M. and V.G.P.; methodology, F.T.R., A.G.M. and E.L.G.; formal analysis, F.T.R., A.G.M. and J.R.M.; investigation, J.R.M., V.G.P., M.I.A., A.G.S., E.L.G., A.G.M., F.T.R., F.J.M.A. and F.S.L.; resources, F.T.R. and J.R.M.; data curation, V.G.P.; writing—original draft preparation, J.R.M., A.G.M., M.I.A., F.T.R., F.J.M.A. and V.G.P.; writing—review and editing, F.S.L.; visualization, J.R.M. and V.G.P.; supervision, J.R.M.; project administration, J.R.M.; funding acquisition, J.R.M. and F.S.L. All authors have read and agreed to the published version of the manuscript.

Funding: This research was funded by "Ministerio de Ciencia, Innovación y Universidades" from the Spanish Government, grant number: RTI2018-096001-B-C33.

Institutional Review Board Statement: Not applicable.

Informed Consent Statement: Not applicable.

Data Availability Statement: Data not available.

Acknowledgments: The authors are grateful to the "Centro de Experiencias Hidrodinámica de El Pardo" (CEHIPAR-INTA) for their experimental work in the calm water towing tank facility.

Conflicts of Interest: The authors declare no conflicts of interest.

References

1. Sanfilippo, F.; Tang, M.; Steyaert, S. Aquatic Surface Robots: The State of the Art, Challenges and Possibilities. In Proceedings of the 2020 IEEE International Conference on Human-Machine Systems (ICHMS), Rome, Italy, 7–9 September 2020; pp. 1–6.
2. Panda, J.P.; Mitra, A.; Warrior, H.V. A review on the hydrodynamic characteristics of autonomous underwater vehicles. *Proc. Inst. Mech. Eng. Part M J. Eng. Marit. Environ.* **2020**, *235*, 15–29. [CrossRef]
3. Alam, K.; Ray, T.; Anavatti, S.G. Design optimization of an unmanned underwater vehicle using low-and high-fidelity models. *IEEE Trans. Syst. Man Cybern. Syst.* **2015**, *47*, 2794–2808. [CrossRef]
4. Alvarez, A.; Bertram, V.; Gualdesi, L. Hull hydrodynamic optimization of autonomous underwater vehicles operating at snorkeling depth. *Ocean Eng.* **2009**, *36*, 105–112. [CrossRef]
5. Ignacio, L.C.; Victor, R.R.; Francisco, D.R.R.; Pascoal, A. Optimized design of an autonomous underwater vehicle, for exploration in the Caribbean Sea. *Ocean Eng.* **2019**, *187*, 106184. [CrossRef]
6. Rashid, M.M.; Roy, R.; Ahsan, M.M.; Siddique, Z. Design and Development of an Autonomous Surface Vehicle for Water Quality Monitoring. *arXiv* **2022**, arXiv:2201.10685. [CrossRef]
7. Odetti, A.; Altosole, M.; Caccia, M.; Viviani, M.; Bruzzone, G. Wetlands Monitoring: Hints for Innovative Autonomous Surface Vehicles Design. In *Technology and Science for the Ships of the Future*; IOS Press: Amsterdam, The Netherlands, 2018; pp. 1014–1022. [CrossRef]
8. Acua Ocean. Ocean Monitoring and Protection. ACUA Ocean Refresh. Available online: https://www.acua-ocean.com (accessed on 19 July 2022).
9. Sanfilippo, F.; Tang, M.; Steyaert, S. The Aquatic Surface Robot (AnSweR), a Lightweight, Low Cost, Multipurpose Unmanned Research Vessel. In *Intelligent Technologies and Applications*; Communications in Computer and Information Science; Yayilgan, S.Y., Bajwa, I.S., Sanfilippo, F., Eds.; Springer International Publishing: Cham, Switzerland, 2021; pp. 251–265. [CrossRef]
10. Torben, T. Hybrid Control of Autonomous Ferries. Project Thesis, Norwegian University of Science and Technology, Trondheim, Norway, 2018. [CrossRef]
11. Jorge, V.A.M.; Granada, R.; Maidana, R.G.; Jurak, D.A.; Heck, G.; Negreiros, A.P.F.; dos Santos, D.H.; Gonçalves, L.M.G.; Amory, A.M. A Survey on Unmanned Surface Vehicles for Disaster Robotics: Main Challenges and Directions. *Sensors* **2019**, *19*, 702. [CrossRef]
12. Khaled, D.; Aly, H.; Khaled, M.; Mahmoud, N.; Shabaan, S.; Abdellatif, A. Development of a Sustainable Unmanned Surface Vehicle (USV) for Search and Rescue Operations. *Int. Undergrad. Res. Conf.* **2021**, *5*, 462–468.

13. Kang, C.M.; Yeh, L.C.; Jie, S.Y.R.; Pei, T.J.; Nugroho, H. Design of USV for Search and Rescue in Shallow Water. In *Intelligent Robotics and Applications*; Lecture Notes in Computer Science; Chan, C.S., Liu, H., Zhu, X., Lim, C.H., Liu, X., Liu, L., Goh, K.M., Eds.; Springer International Publishing: Cham, Switzerland, 2020; pp. 351–363.
14. Liu, Z.; Zhang, Y.; Yu, X.; Yuan, C. Unmanned surface vehicles: An overview of developments and challenges. *Annu. Rev. Control.* **2016**, *41*, 71–93. [CrossRef]
15. Liu, D.-Y.; Gao, X.-P.; Huo, C. Motion planning for unmanned surface vehicle based on a maneuverability mathematical model. *Ocean Eng.* **2022**, *265*, 112507. [CrossRef]
16. Wang, X.; Deng, Z.; Peng, H.; Wang, L.; Wang, Y.; Tao, L.; Lu, C.; Peng, Z. Autonomous docking trajectory optimization for unmanned surface vehicle: A hierar-chical method. *Ocean. Eng.* **2023**, *279*, 114156. [CrossRef]
17. Mousazadeh, H.; Jafarbiglu, H.; Abdolmaleki, H.; Omrani, E.; Monhaseri, F.; Abdollahzadeh, M.-R.; Mohammadi-Aghdam, A.; Kiapei, A.; Salmani-Zakaria, Y.; Makhsoos, A. Developing a navigation, guidance and obstacle avoidance algorithm for an Unmanned Surface Vehicle (USV) by algorithms fusion. *Ocean Eng.* **2018**, *159*, 56–65. [CrossRef]
18. Liang, X.; Qu, X.; Hou, Y.; Li, Y.; Zhang, R. Distributed coordinated tracking control of multiple unmanned surface vehicles under complex marine environments. *Ocean Eng.* **2020**, *205*, 107328. [CrossRef]
19. He, S.; Dong, C.; Dai, S.-L. Adaptive neural formation control for underactuated unmanned surface vehicles with collision and connectivity constraints. *Ocean Eng.* **2021**, *226*, 108834. [CrossRef]
20. Huang, B.; Song, S.; Zhu, C.; Li, J.; Zhou, B. Finite-time distributed formation control for multiple unmanned surface vehicles with input saturation. *Ocean Eng.* **2021**, *233*, 109158. [CrossRef]
21. Meng, L.; Zhang, W.; Quan, D.; Shi, G.; Tang, L.; Hou, Y.; Breitkopf, P.; Zhu, J.; Gao, T. From topology optimization design to additive manufacturing: Today's success and tomorrow's roadmap. *Arch. Comput. Methods Eng.* **2019**, *27*, 805–830. [CrossRef]
22. Zhu, J.; Zhou, H.; Wang, C.; Zhou, L.; Yuan, S.; Zhang, W. A review of topology optimization for additive manufacturing: Status and challenges. *Chin. J. Aeronaut.* **2021**, *34*, 91–110. [CrossRef]
23. Wu, F.; Lian, H.; Pei, G.; Guo, B.; Wang, Z. Design and optimization of the variable-density lattice structure based on load paths. *Facta Univ. Series Mech. Eng.* **2023**, *21*, 273–292. [CrossRef]
24. Brizzolara, S.; Curtin, T.; Bovio, M.; Vernengo, G. Concept design and hydrodynamic optimization of an innovative SWATH USV by CFD methods. *Ocean Dyn.* **2011**, *62*, 227–237. [CrossRef]
25. Guan, G.; Wang, L.; Geng, J.; Zhuang, Z.; Yang, Q. Parametric automatic optimal design of USV hull form with respect to wave resistance and seakeep-ing. *Ocean. Eng.* **2021**, *235*, 109462. [CrossRef]
26. Prasad, B.; Dhanak, M. Hydrodynamics of Advanced-Hull Surface Vehicles. In Proceedings of the OCEANS 2018 MTS/IEEE Charleston, Charleston, SC, USA, 22–25 October 2018; pp. 1–7. [CrossRef]
27. Setiawan, J.D.; Septiawan, M.A.; Ariyanto, M.; Caesarendra, W.; Munadi, M.; Alimi, S.; Sulowicz, M. Development and Performance Measurement of an Affordable Unmanned Surface Vehicle (USV). *Automation* **2022**, *3*, 27–46. [CrossRef]
28. *ISO/ASTM 52910:2018*; Additive Manufacturing Design Requirements, Guidelines and Recommendations. ISO/ASTM International: Geneva, Switzerland, 2018.
29. Pei, E.; Kabir, I.R.; Leutenecker-Twelsiek, B. History of AM. In *Springer Handbook of Additive Manufacturing*; Pei, E., Bernard, A., Gu, D., Klahn, C., Monzón, M., Petersen, M., Sun, T., Eds.; Springer International Publishing: Cham, Switzerland, 2023; pp. 3–29. [CrossRef]
30. University of Maine: 3Dirigo', Maine Boats Homes & Harbors. Available online: https://maineboats.com/print/issue-162/university-maine-3dirigo (accessed on 9 November 2023).
31. Moi. Composites Production Made Simple. Available online: https://www.moi.am/projects/mambo (accessed on 9 November 2023).
32. Renau, J.; Tejada, D.; García, V.; López, E.; Domenech, L.; Lozano, A.; Barreras, F. Design, development, integration and evaluation of hybrid fuel cell power systems for an unmanned water surface vehicle. *Int. J. Hydrog. Energy* **2024**, *54*, 1273–1285. [CrossRef]
33. Silva, I.S.; Campopiano, F.; Lopes, G.S.; Uenojo, A.K.; Silva, H.T.; Pellini, E.L.; Alvarez, A.A.; Barros, E.A. Development of a Trimaran ASV. *IFAC-PapersOnLine* **2018**, *51*, 8–13. [CrossRef]
34. Zhu, J.; Chen, L. A probabilistic multi-objective design method of sail-photovoltaic-hybrid power system for an unmanned ocean surveillance trimaran. *Appl. Energy* **2023**, *350*, 121604. [CrossRef]
35. Daidola, J.C.; Arnold, A.M.; Imbesi, M.J. Trimaran Preliminary Structural Design Procedures for a Large High Speed Sealift Ship. *Nav. Eng. J.* **2017**, *129*, 113–121.
36. Tang, H.; Ren, H.; Zhong, Q. Design and model test of structural monitoring and assessment system for trimaran. *Brodogradnja* **2019**, *70*, 111–134. [CrossRef]
37. Jia, D.; Li, F.; Zhang, C.; Li, L. Design and simulation analysis of trimaran bulkhead based on topological optimization. *Ocean Eng.* **2019**, *191*, 106304. [CrossRef]
38. Khoob, A.A.; Ketabdari, M.J. Short-term prediction and analysis of wave-induced motion and load responses of a wave-piercing trimaran. *Brodogradnja* **2020**, *71*, 123–142. [CrossRef]
39. Ghadimi, P.; Nazemian, A.; Ghadimi, A. Numerical scrutiny of the influence of side hulls arrangement on the motion of a Trimaran vessel in regular waves through CFD analysis. *J. Braz. Soc. Mech. Sci. Eng.* **2018**, *41*, 1. [CrossRef]
40. Dogrul, A.; Yildiz, B. Numerical Prediction of Form Factor and Wave Interference of a Trimaran for Different Outrigger Positions. *China Ocean Eng.* **2022**, *36*, 279–288. [CrossRef]

41. Khoob, A.A.; Feizi, A.; Mohamadi, A.; Vakilabadi, K.A.; Fazeliniai, A.; Moghaddampour, S. An experimental study on the effect of the side hull symmetry on the resistance performance of a wave-piercing trimaran. *J. Mar. Sci. Appl.* **2021**, *20*, 456–466. [CrossRef]
42. Wang, S.; Duan, W.; Xu, Q.; Duan, F.; Deng, G.; Li, Y. Study on fast interference wave resistance optimization method for trimaran outrigger layout. *Ocean Eng.* **2021**, *232*, 109104. [CrossRef]
43. Tang, H.; Zhang, X.; Ren, H.; Yu, P. Numerical study of trimaran motion and wave load prediction based on time-domain Rankine-Green matching method. *Ocean Eng.* **2020**, *214*, 107605. [CrossRef]
44. Xu, X.Y.; Meng, C.Y.; Wang, K. Resistance performance forecast of trimaran based on multiple regression analysis. *E3S Web Conf.* **2021**, *261*, 02072. [CrossRef]
45. Yao, C.; Dong, G.; Sun, X.; Zheng, Y.; Feng, D. Numerical study on motion and added resistance of a trimaran advancing in waves based on hybrid Green function method. *Appl. Ocean Res.* **2023**, *130*, 103432. [CrossRef]
46. Liao, X.; Chen, Z.; Gui, H.; Du, M. CFD prediction of ship seakeeping and slamming behaviors of a trimaran in oblique regular waves. *J. Mar. Sci. Eng.* **2021**, *9*, 1151. [CrossRef]
47. Gong, J.; Li, Y.; Fu, Z.; Li, A.; Jiang, F. Study on the characteristics of trimaran seakeeping performance at various speeds. *J. Braz. Soc. Mech. Sci. Eng.* **2021**, *43*, 194. [CrossRef]
48. Wang, S.; Ma, S.; Duan, W. Seakeeping optimization of trimaran outrigger layout based on NSGA-II. *Appl. Ocean Res.* **2018**, *78*, 110–122. [CrossRef]
49. Zong, Z.; Hong, Z.; Wang, Y.; Hefazi, H. Hull form optimization of trimaran using self-blending method. *Appl. Ocean Res.* **2018**, *80*, 240–247. [CrossRef]
50. Nazemian, A.; Ghadimi, P. CFD-based optimization of a displacement trimaran hull for improving its calm water and wavy condition resistance. *Appl. Ocean Res.* **2021**, *113*, 102729. [CrossRef]
51. Nazemian, A.; Ghadimi, P. Global optimization of trimaran hull form to get minimum resistance by slender body method. *J. Braz. Soc. Mech. Sci. Eng.* **2021**, *43*, 67. [CrossRef]
52. Sun, C.; Guo, C.; Wang, C.; Wang, L.; Lin, J. Numerical and experimental study of flow field between the main hull and demi-hull of a trimaran. *J. Mar. Sci. Eng.* **2020**, *8*, 975. [CrossRef]
53. Jiang, Y.; Sun, H.; Zou, J.; Hu, A.; Yang, J. Experimental and numerical investigations on hydrodynamic and aerodynamic characteristics of the tunnel of planing trimaran. *Appl. Ocean Res.* **2017**, *63*, 1–10. [CrossRef]
54. Jiang, J.; Ding, J.; Gong, J.; Li, L. Effect of hull displacement on hydro- & aerodynamics of a planing trimaran. *Appl. Ocean Res.* **2022**, *120*, 103050. [CrossRef]
55. Ding, J.; Jiang, J. Tunnel flow of a planing trimaran and effects on resistance. *Ocean Eng.* **2021**, *237*, 109458. [CrossRef]
56. Giménez, A.; Martínez, M.; Renau, J.; García, V.; Domenech, L.; Ibáñez, M.; Real, A.; Cortés, E.; Šakalyté, A.; García, J.A.; et al. Polymer-Based Interface Optimization for Coated Lightweight Composites Additive Manufacturing. In Proceedings of the 20th European Conference on Composite Materials, Lausanne, Switzerland, 26–30 June 2022; pp. 647–654.